Available online at www.sciencedirect.com

ScienceDirect

Procedia Engineering 68 (2013) 431 – 438

Procedia Engineering

www.elsevier.com/locate/procedia

The Malaysian International Tribology Conference 2013, MITC2013

Biodegradability of nanoparticle modified fiber reinforced polyester resin nanocomposite

M.N.K. Chowdhury[a], M.D.H. Beg[a]*, Maksudur R. Khan[a]

[a]*Faculty of Chemical and Natural Resources Engineering, Universiti Malaysia Pahang, 26300, Gambang, Kuantan, Pahang, Malaysia.*

Abstract

Copper nanoparticles (CuNPs) have been synthesized under chemical reduction and in aqueous medium where polyvinyl alcohol (PVA) played a role as a stabilizer. From Transmission electron microscopy (TEM) images analysis, calculated average size of the synthesized CuNPs was 3.5 nm. The synthesized CuNPs were loaded in the oil palm empty fruit bunch (EFB) natural fibers. Surface of the fibers were modified by cationic agent (CA). The existance of hydroxyl group in fibres exhibit negative charge and inhibit the PVA surrounded negatively charged on CuNPs. Several types of composites were developed using hand mixing process by varying the fiber types. The developed composites were formulated using untreated empty fruit bunch fibers (UF) and CuNPs loaded EFB fibers (NF) with commercially available unsaturated polyester resin (UPER). The UF, NF, UPER and nanocomposites were characterized by Fourier transform infrared spectroscopy (FTIR), field emission scanning electron microscopy (FESEM), x-ray diffactometer (XRD), differential scanning calorimetry (DSC), tensile strength test, etc. The results from biodegradation study showed that significant weight loss was not observed for virgin resin (VR) and VR-NF nanocomposite whereas, the VR-UF composite showed ca. 13.3% weight loss at 90 days, reflected to preferential degradation of the natural fibers.

Selection and peer-review under responsibility of The Malaysian Tribology Society (MYTRIBOS), Department of Mechanical Engineering, Universiti Malaya, 50603 Kuala Lumpur, Malaysia

Keywords: Nanoparticle; Natural fiber; Polyester resin; Nano-composite; Biodegradability;

Nomenclature

D	Crystallite size (nm)
I	Intensity
Greek symbols	
θ	diffraction angle (degree)
λ	wave length of X-ray (Angstrom)
β	FWHM (radians)
Subscripts	

* Corresponding author. Tel.: +6-095-49-2816; fax: +6-095-49-2889.
E-mail address: dhbeg@yahoo.com

Selection and peer-review under responsibility of The Malaysian Tribology Society (MYTRIBOS), Department of Mechanical Engineering, Universiti Malaya, 50603 Kuala Lumpur, Malaysia
doi:10.1016/j.proeng.2013.12.203

hkl	Coordinates
am	amorphous

1. Introduction

Fiber–reinforced plastic composites have played a potential role due to a variety of applications for their high specific strength and modulus. The traditional fiber–reinforced plastics are usually made up of synthetic fiber–reinforced composites, which are considered critically and because of their environmental complications such materials are less popular. Recently, the interest is growing for alternatives which are the natural fibers based biodegradable plastic composites [1–4]. The benefits of natural fibers are: biodegradability, renewability, low cost, and low density. This light fiber can give superior specific stiffness and strength that are analogous to the respective synthetic fibers like glass fibers. The promising applications of natural fiber reinforced composites: door, package trays, instrument panels, arm rest, seat back and glove boxes [1]. However, the drawbacks of natural fibers are the high degree of moisture absorption, poor wettability with non-polar polymers, low-adhesion of untreated fibers with polymer–matrix facilitates the retardation of significant bonding during aging [3–5]. To seize these difficulties the promising methods are the fabrication of fiber, cautious choice of pair (fiber and matrix), and advance development procedures [6, 7].

Many natural fibers such as kenaf , flax, and jute are using as reinforcements for plastic composite materials [1–4]. With these, oil palm empty fruit bunch (EFB) fibers are also popular for the same functioning. EFB fiber is mainly a cellulosic materials and an abundant renewable biomass in some countries like Malaysia, Indonesia, India, Brazil, etc. However, this biomass still remains less important even though they have environmentally friendly and biocompatible features. Consequently, improvement of mechanical and antibacterial performance of EFB fibers using facile approach attracts many researchers. To exhibit a broad-spectrum biocide and inhibition of the growth of bacteria, fungi and algae, Cu is very prominent. Hence, the present work has been undertaken to synthesize CuNPs, which, is then embedded in EFB fibers, to make them strong and durable. This strong and durable fibers can be exploited in due applications especially for nanocomposite, which may be suggested for many value-added industrial products such as automotive, agriculture and other industrial sectors [8]. Especially, it is the first time attempt has been made to study the properties of CuNPs loaded EFB fiber–reinforced unsaturated polyester resin (UPER) composites. Prior to the loading of CuNPs in fibers, the surface of them are modified by the cationic agent (CA) to ensure the optimum impregnation [9]. Thereafter, several kinds of composite were developed; characterized through FTIR, FESEM, XRD, DSC, tensile strength tests, etc. and the materials properties are studied

2. Experimental

2.1. Materials

Copper chloride dihydrate salt with 98 % purity and analytical grade sodium hydroxide were procured from ALDRICH. Polyvinyl alcohol (PVA) (MW = 30,000 –70,000), sodium borohydride (purity 99 %), ascorbic acid (purity 99.7 %) and 60% solution of (3-Chloro-2-hydroxypropyl)trimethylammonium chloride (CA) solution were purchased from ALDRICH. Raw EFB fibers (average density = 1.1868 g/cm^3) were collected from the LKPP Corporation Sdn. Bhd., Kuantan, Malaysia. Unsaturated polyester resin (268BQT, commercial grade) obtained from PERMULA Chemicals SDN BHD. 2-Butanone peroxide (ALDRICH) was used as cross-linker.

2.2. Methods

The raw fibers of golden-brown color with an average diameter of 0.175 ± 0.071 mm were washed to remove dust particles and dried under sunlight for 3 days. The fibers thus obtained were referred to untreated EFB fibers (UF).

CuNPs were synthesized in 0.5% PVA solution with deionized (DI) water. Copper chloride (250 mg) and ascorbic acid (20 times with respect to the precursor molar ratio) were subsequently added in 100 mL PVA solution with vigorous stirring. About 7.0 mL solution of sodium borohydride (0.347 M) was injected drop-wise to the above-mentioned reaction mixture with continuous stirring for 2 h for the preparation of CuNPs sols. The UF fibers were dipped in 20% CA solution by maintaining a liquor ratio of 1:25 in a water bath for cationization reaction. During the cationization process, the bath was set at a constant temperature of 60 ^{o}C along with continuous agitation. Thereafter, 15% sodium hydroxide (40 g/L) with respect to the fiber-weight was added in three steps at an interval of 5 min, and the mixture was further stirred for 15 min.

The cationized EFB (CF) fibers were removed from the bath, rinsed several times with water, neutralized and then dried at the ambient temperatures. The CF fibers were introduced in the synthesized CuNPs sols of copper concentration 250 mg/L, maintaining the fiber to sol ratio of 1:25 with continuous shaking by a mechanical shaker for 12 h. Then, the CuNPs reinforced CF (NF) fibers were removed from the bath, rinsed with water, and dried in the dark place at room temperature.

Fourier-transformed infrared (FTIR) spectra of liquid samples were taken with a PerkinElmer Spectrum 100 FTIR Spectrometer over the frequency range 4000–650 cm^{-1}. On the other hand, FTIR spectra of different solid samples were recorded over the same frequency range using a Thermo Scientific Model Smart Performer attenuated total reflectance (ATR) accessory of Ge crystal, attached to a Thermo Scientific spectrophotometer (Model Nicolet Avatar-370) with a single bounce. The degree of cationization (C_d) was calculated according to the following relation [9]:

$$C_d = \{(I_{1648} - I_{1495})/ I_{1648}\} \times 100 \quad (1)$$

where I_{1648} and I_{1495} are the maximum intensities of peak at 1648 and 1495 cm^{-1}, respectively.

Transmission electron microscopy (TEM) was performed by a LEO 912 AB EFTEM operating at 120 kV to monitor the size of nanoparticles. Treated and untreated EFB fiber (UF) surface were investigated by using a scanning electron microscope (SEM) of model ZEISS, EVO50, Germany. Surface morphologies of fibers were also investigated by using a field emission scanning electron microscope (FE-SEM) of JEOL JSM-7600F, USA, equipped with an energy dispersive X-ray (EDX) system (OXFORD INCA. Fibers were mounted on sample holders with carbon tape and sputtered by platinum.

X-ray diffraction (XRD) data were collected by using a RigakuMiniFlex II (30 kV and 15 mA), Japan, equipped with computer-controlled software to set up the apparatus and analyze the data. The average size of the cellulose crystallites, D_{hkl}, was determined with the full width at half-maximum (FWHM) of the (002) peak by using the following Scherer formula:

$$D_{hkl} = (0.9\,\lambda/\beta\cos\theta) \quad (2)$$

where, β is the FWHM (in radians) and θ is the diffraction angle.

The X-ray crystallinity, Crl(%) , was calculated by the help of Segal's method with the following equation [10]:

$$Crl(\%) = \{(I_{002} - I_{am})/I_{002}\} \times 100 \quad (3)$$

where I_{002} is the maximum intensity of 002 (at $2\theta \approx 22°$) reflections from the crystalline and amorphous components, and I_{am} (at $2\theta \approx 16°$)is the minimum intensity of diffraction from the amorphous part of EFB fibers.

The single EFB fibers were subjected to the ASTM D3379-75 standard test method for tensile strength. The single fibers were individually placed in the grips of a DIA-STRON LTD/U.K (FDAS 765) tensile testing machine, and the supporting sides of the paper were carefully cut to maintain the gauge length of 30 mm, at a rate of 3

mm/min using a 500 N-load cell. Average strength was obtained using from 50 specimens. The tensile tests of composites were carried out using the same machine as according to the standard methods ASTM D3039. The used wt.% of fiber was 30% which was optimized and so it was used. The crosshead speed of the tensile testing was set at 3 mm/min. The dimension for tensile specimen is 60 mm long and 13 mm wide. All the results were taken as the average value of twenty samples.

Differential scanning calorimetry (DSC) was performed to determine the glass transition temperature (T_g), melting temperature (T_m) and crystallization temperature (T_c), using a TA/Q1000 apparatus under nitrogen atmosphere.

Biodegradability was determined by measuring the weight loss of the specimens which are buried in soil. The test was done by using the soil of 1:1 mixture of black soil and leaf mold for gardening. The selected each specimen was buried in the aforesaid soil and incubated at room temperature (25–30 °C). At two days intervals, water was poured so that the soil was kept in humid condition. After burial of particular time the specimens were exposed from the soil, where the burial duration followed for 30, 60 and 90 days, respectively. Thereafter, the specimens were washed with water and dried at 40 °C in a vacuum oven up to a constant weight. The weight loss (%) is calculated according to the following formula:

$$\text{Weight loss (\%)} = \{(W_i - W_f)/W_f\} \times 100 \quad (4)$$

where W_i and W_f are the dry weights of composites at the before and after the burial, respectively.

3. Results and discussion

Due to the addition of reducing agent, a clear change of sol color is observed, where the light-blue colored aqueous solution changes to wine red, which is a considerable indication of the formation of CuNPs in the sol. In addition, Fig. 1(i) illustrates the FTIR spectra of solutions before and after CuNPs formation. A broad absorption band of hydroxyl (O–H) groups of PVA chains appear at 3359 cm^{-1} and 3341 cm^{-1} before and after nanoparticles (NPs) formation, respectively, showing 18 units red shift of this polar group. This shifting of wavenumber demonstrates that PVA molecules facilitate coordination with Cu^{2+} species. Such coordination through the ester bond of PVA to Cu species due to the electrostatic attractions was described elsewhere [11]. The ester bond is located at 1047 cm^{-1} before NPs formation and shifted to 1039 cm^{-1} after NPs formation, indicating the coordination of polar -O-H groups with Cu species.

The morphologies and sizes of CuNPs in the sol were observed by TEM as shown in Fig. 1(ii), where the developed NPs in the sol are in sizes in the order of 1.2–10.5 nm (average size of 3.5±1.1 nm) with spherical shape. The morphologies and sizes of CuNPs were also observed by FESEM and XRD, respectively.

The adsorptions of CuNPs on CF fibers measured by EDX also (shown in EDX spectrum of Fig. 2(b)). Actually, when CF fibers are immersed in CuNPs sol; where, CuNPs stabilized by negatively charged PVA spheres can readily be adsorbed by the positive sites of CF. At the fiber surface, a large number of negative charges were reduced because of cationization of fibers, thereby increasing the adsorption capability of functionalized copper nanoparticles due to an attractive interaction between CF and CuNPs.

The X-ray diffractograms of different fibers are illustrated in Fig. 3(i). The peak appearing at $2\theta=42.3°$ for NF has been reportedly attributed to the 111 reflection from the cubic copper crystal [12]. This finding demonstrates the CuNPs impregnation in the fibers. The average size of CuNPs as analyzed from (1 1 1) peak is ~17 nm.

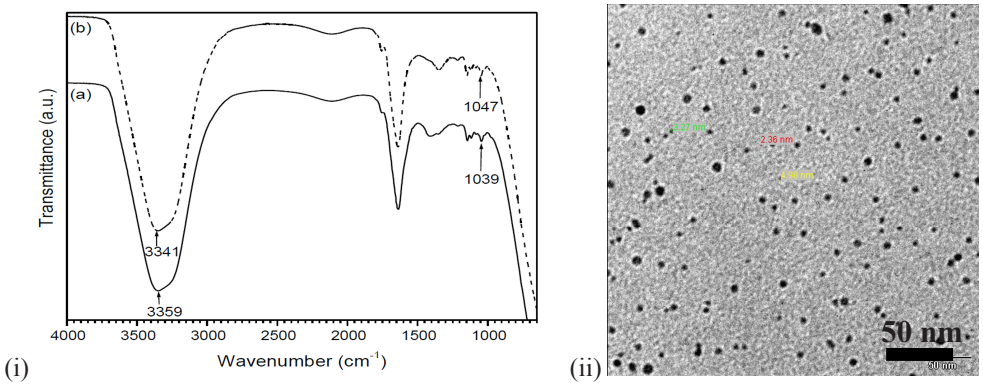

Fig. 1. (i) FTIR spectra of sols: (a) before and (b) after CuNPs formation, (ii) TEM image of synthesized CuNPs.

Table 2 represents the mechanical performances (*TS*) of different fibers in different conditions before burial (BB) and after burial (AB) under soil. Analyses show that the increase in TS of NF fiber from UF fiber before burial is 25%. This increase in TS is rational, because the functionalized CuNPs can enter into fiber matrices and act as filler or plasticizer, which contribute to load sharing during stretching the fibers. On the other hand, the TS of UF and NF after soil burial decreases by 32% and 25% from their respective TS before burial, resulting in 7% antifungal activity. However, the TS-decrease of UF fibers is more than NF fibers, demonstrating that CuNPs reinforced fibers are more durable than the control ones. This fact is due to the metallic CuNPs can show a certain degree of sterilization, because the catalytic properties of metallic species partly help to create active oxygen in water, which dissolve the organic substances to maintain sterilizing effect [13].

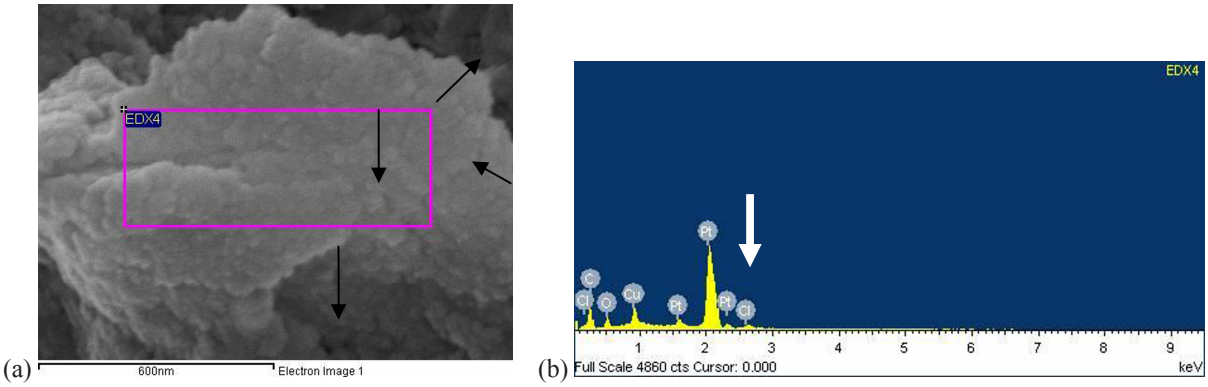

Fig. 2. (a) FESEM image of loaded CuNPs (arrow marked) in CF, (b) EDX spectrum of the pink box area (shown in (a)) of CF.

Fig. 3(ii) represents the FTIR spectra of (a) VR, (b) NF-VRC. The major absorbance peaks obtained for the VR are: (a) the peak around 3450 cm^{-1}, which may be attributed to the OH stretching, (b) the strong peaks at 3089 and 2976 cm^{-1} that can be assigned to the C–H stretching in aromatic and aliphatic moieties, respectively, (c) the C=O stretching (from ester linkage) observed at 1732 cm^{-1}, also observed at 1955 cm^{-1} [14] (d) the CH_2 deformation appearing at 1450 cm^{-1}, and (e) the C–O asymmetric mode of the ester groups observed at 1073 cm^{-1}. The FTIR spectrum of NF-VRC also indicates the presence of aforesaid functional groups absorption frequencies with some shifting in some important positions. The crucial changes of peak at 1955 cm^{-1} is almost invisible in the spectrum of

Fig. 3(ii) (spectrum b) as well as the significant red shift occurred for C=O and C–O groups from ester moiety. These observed findings are indicating the significant degree of bonding among the components of composites.

The DSC parameters from thermograms of VR and NF-VRC are shown in Table 1. On heating, the pure VR displays three main successive transitions: a glass transition, a cold crystallisation exotherm and a melting endotherm, which are respectively characterized by temperatures T_g, T_c and T_m. The presence of single melting peak of the composites is due to the existence of single phase of composite, developed during the controlled cooling process in the presence of NP-CF fibers [15]. In table 1, the T_g value of VR in the NF-VRC decreases. This fact can be explained on the basis of the polymer chain mobility, which is easier in VR as compared to NF-VRC, because the higher crystallinity for the latter, as obvious from the XRD study, is a strong evidence for more restrictions of chain movement. The T_c decreases significantly for composites, as VR > NF-VRC. Interestingly, changes of melting endotherm of composites are also displayed the similar outline.

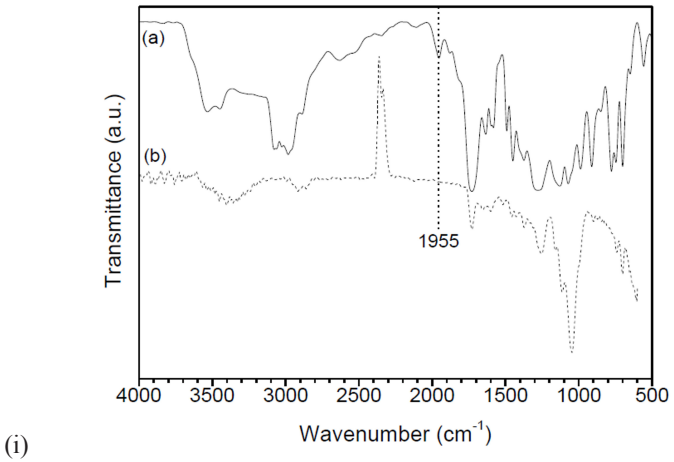

(i)

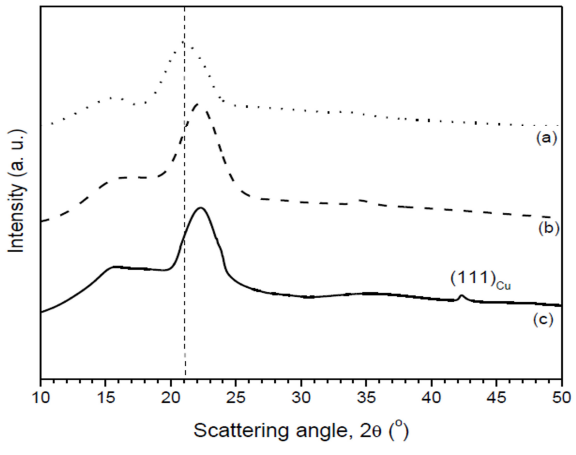

(ii)

Fig. 3. (i) XRD patterns of different fibers: (a) UF, (b) CF, and (c) NF, and (ii) FTIR spectra of (a) VR and (b) NF-VRC.

The most important factor to obtain a good fiber reinforced composites is the adhesion between matrix polymers or the fiber and interphase properties. Due to the presence of hydroxyl group in natural fibers, the moisture absorption is high which leads to poor wettability and weak interfacial bonding between fibers and hydrophobic

matrices. Therefore, in order to develop composites with better mechanical properties, it is necessary to impart hydrophobicity to the fibers by suitable modification [16].

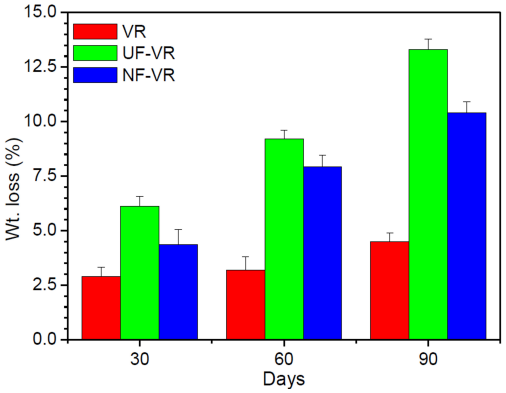

Table 1. Parameters from DSC analysis

Parameters	VR	NF-VRC
T_g (°C)	75.5	67.5
T_c (°C)	150	139.8
T_m (°C)	171.4	148

Table 2. Tensile strength (TS) results from soil burial test

Fibres	UF		NF	
State	BB	AB	BB	AB
TS (MPa)	259	176	347	261

Fig. 4Biodegradability of VR and different composites under soil burial.

The surface modification of UF would not only decrease the moisture absorption, but would improve the wettability of fiber and matrix at interphase region hence subsequently improves the mechanical properties of the composites. The tensile properties of the resin at 0 wt.% of fiber (i.e., virgin resin, (VR)) is used as control. It is observed that the use of 30 wt.% NF, performed the improved tensile properties compare of the VR composites. The superior mechanical properties of NF based composites as compared to UF composites are attributed to the fact that treatment improves the fiber surface adhesives characteristics by fibrillation process [17].

The weight loss increased with burial-time for all the specimens and the results are shown in Fig. 4. Significant difference observed between VR and NF-VRC samples at 90 days. The UF-VRC specimen buried for more than 60 days could not be fully recovered because of a considerable fragmentation. Apparent decay of neat VR and NF-VRC is slower than that of UF-VR, indicating that UF has a higher biodegradability than NF. This phenomenon is logical due to the achievement of strong and durable properties of NF. Cautious observation reveals that some hollows generated by the biodegradation of matrix VR are appeared for all the VR samples after 30 days. The biodegradability of matrix polymer is thought to be almost the same for all the samples, as far as judging from the growth of hollows of the matrix VR. It is thought that the faster fragmentation of UF-VRC is caused by a rapid biodegradation of UF exposed on the surface by the biodegradation of the matrix VR.

Table 3 represents the TS of VR, UF-VRC, and NF-VRC at different conditions. Clearly, NF-VRC showed the highest TS, which are immediately followed by UF-VRC. The respective increase of TS of NF-VRC from UF-VRC is about 27%, and from VR is 58%, denoting a significant figure to enhance materials properties. This better performance of the resulting composites can be attributed to the increased compatibility between NP-CF fibers and VR because of the modification of UF fibers surface by both CA and CuNPs treatments. On the other hand, the increase of TS in the composites merely for the inclusion of UF fibers content may be assigned to the robust TS value of the individual EFB fiber [18]. However, when UF fiber content is greater than 30 wt%, the composites become inhomogeneous because of the fiber–fiber interaction whose effect may cause to develop fiber-agglomeration in the composites, as reported elsewhere [19].

Table 3. Tensile strength results of virgin resin and different fiber reinforced composites.

Sample	TS (before soil burial) (MPa)	TS (after soil burial) (MPa)	% of changes
VR	19±2.2	11±1.4	-42
UF-VRC	33±4.3	21±2.7	-36
NF-VRC	45±4.7	37±4.1	-18

4. Conclusion

CuNPs have been synthesized at ambient conditions which were loaded in UF via cationization with CA. FTIR result has confirmed the 36% cationization. FESEM and XRD analyses for NF revealed that CuNPs were impregnated in the fiber which can improve the strength and durability of the fibers. The developed NF-VRC has good mechanical performances and controlled biodegradability. For NF-VRC, the obtained results from FTIR, DSC and 12% decrease of T_g, are pointed out a substantial enhancement of materials properties by NF. FTIR spectroscopy has provided strong evidence for bond formation among the components of NF-VRC. Furthermore, findings observed from DSC and X-ray diffraction have been consistent. The new material studied has potential for usable materials in replace of different particle boards.

Acknowledgements

Authors would like to acknowledge Universiti Malaysia Pahang, Malaysia for providing financial support through GRS110322 and RDU120106 for this project.

References

[1] Hall, D.B., Underhill, P., Torkelson, J.M., 1998. Spin coating of thin and ultrathin polymer films, Polym. Eng. Sci. 38, pp, 2039–2045.
[2] Miller, A.F., 2009. Exploiting wrinkle formation, Science 317, pp. 605–606.
[3] Rotella, C., Napolitano, S., Wulbbenhorst, M., 2009. Segmental mobility and glass transition temperature of freely suspended ultrathin polymer membranes, Macromolecules 42, pp. 1415–1417.
[4] Tsukruk, V.V., 1997. Assembly of supramolecular polymers in ultrathin films, Prog Polym Sci, 22, pp. 247–311.
[5] Pérez, L.D., López, J.F., Orozco, V.H., Kyu, T., López, B.L., 2009. Effect of the chemical characteristics of mesoporous silica MCM-41 on morphological, thermal, and rheological properties of composites based on polystyrene, J Appl Polym Sci, 111, pp. 2229–2237.
[6] Vargas, A.F., Brostow, W., Hagg Lobland, H.E., Lopez, B.L., Olea-Mejia, O., 2009. Reinforcement of polymeric latexes by in situ polymerization, J Nanosci Nanotechnol 9, pp. 6661–6667.
[7] Zou, H., Wu, S., Shen, J. 2008. Polymer/Silica Nanocomposites: Preparation, characterization, properties, and applications, Chem Rev 108, pp. 3893–3957.
[8] Jiang, C., Markutsya, S., Pikus, Y., Tsukruk, V.V., 2004. Freely suspended nanocomposite membranes as highly sensitive sensors, Nat Mater 3, pp. 721–728.
[9] Chowdhury, M. N. K., Beg, M. D. H., Maksudur R. K., Mina, M. F., 2013. Modification of oil palm empty fruit bunch fibers by nanoparticle impregnation and alkali treatment, Cellulose 20, pp. 1477–1490.
[10] Inagaki, T., Siesler, H. W., Mitsui, K., Tsuchikawa, S., 2010. Difference of the crystal structure of cellulose in wood after hydrothermal and aging degradation: a NIR spectroscopy and XRD study, Biomacromolecules 11, pp. 2300–2305, July 2010.
[11] Zhang, H.X., Siegert, U., Liu, R., Cai, W.B., 2009. Facile fabrication of ultrafine copper nanoparticles in organic solvent, Nanoscale Res Lett, vol.4, pp. 705–708.
[12] Xie, W.Y.H., Chen, L., Li, Y., Zhang, C., 2009. Synthesis and characterization of monodispersed copper colloids in polar solvents, Nanoscale Res Letters 4, pp. 465–470.
[13] Chowdhury, M. N. K., Beg, M. D. H., Maksudur R. K., Mina, M. F., 2013. Synthesis of copper nanoparticles and their antimicrobial performances in natural fibers, Materials Letters 20, pp. 26–29.
[14] Dutta, A., Hamilton, G. A., Hartnett, H. E.,. Jones, A. K., 2012. Construction of Heterometallic Clusters in a Small Peptide Scaffold as [NiFe]-Hydrogenase Models: Development of a Synthetic Methodology, Inorg. Chem. 51, pp. 9580−9588.
[15] Pluta, M., Galeski, A., 2002. Crystalline and supermolecular structure of polylactide in relation to the crystallization method, J Appl Polym Sci, 86, pp. 1386–1395.
[16] Vilay, V., Mariatti, M., Mat Taib, R., Mitsugu Todo, 2008. Effect of fiber surface treatment and fiber loading on the properties of bagasse fiber–reinforced unsaturated polyester composites, Composites Science and Technology 68, pp. 631–638.
[17] Vazquez, A., Dominguez, V.A., 1999. Bagasse fiber-polypropylene based composites, J Thermoplast Compos Mater, pp. 12.
[18] Shinji. Ochi,, 2008. Mechanical properties of kenaf fibers and kenaf/PLA composites, Mech Mater, 40, pp. 446–452.
[19] Joseph, S., Joseph, K., Thomas, S., 2006. Green composites from natural rubber and oil palm fiber: physical and mechanical properties, Int J Polym Mater 55, pp. 925–945.